Transactions on Energy Systems and Engineering Applications

Article

Investigating the impact of diverse PIDs and ESDs in frequency regulation of a wind-diesel hybrid system

Vikash Rameshar[1], Gulshan Sharma[1,*] and Pitshou N. Bokoro[1]

[1] Department of Electrical & Electronics Engineering Technology, University of Johannesburg, Johannesburg 2094, South Africa

[*] Correspondence: gulshans@uj.ac.za

Received: 12 March 2024; Accepted: 16 May 2025; Published: 16 September 2025

Abstract: Microgrids are gaining momentum these days as they can generate the cleaner and affordable electrical energy through renewable energy sources. The renewable energy sources such as wind has enough potential. However, its operation is restricted as wind speed highly varies over the period of the day and that is why diesel engine generation is a possible solution to overcome the wind challenges as well as to supply the uninterrupted electrical energy to the customers. This paper presents the design of various PID controllers to match the energy generation with load demand and hence to stabilize the operation of the microgrid for various operating conditions. The performance of the PID controllers is obtained through gains calculation, diverse error values and through dynamic responses of the microgrids obtained through diverse controllers. Further, this paper also shows the impact of diverse energy storage devices (ESD) with PID controllers for the microgrid, and it is observed that PIL-PID with redox flow battery outperform other controllers and ESDs and most suited for various working conditions of the microgrid.

1. Introduction

Some of the clean renewable energy sources such as biogas, solar power (SPV), wind power and biogas come under the category of renewable energy sources (RES). Sun-radiated technology, such as SPV and wind power the facilities, has been dominant, and a mix of diesel, wind, and thermal provides benefits and advantages in the RES market. Additionally, it boosts economic growth financially and the development of communities [1–4]. With the promotion of RES systems toward positive economic growth, one needs to stick to the management and prominence of the electricity produced by the systems and how they progress if the RES are applied within the energy system. Due to the challenges linked with fossil fuels depletion, such as increased costs and shortages, which promotes a beneficial development regarding RES to support the control systems. Renewable energy power systems also bring about issues such as frequency deviations

How to cite this article: Rameshar, Vikash; Sharma, Gulshan; Bokoro, Pitshou. Investigating the impact of diverse PIDs and ESDs in frequency regulation of a wind-diesel hybrid system. *Transactions on Energy Systems and Engineering Applications*, 6(2): 648, 2025. DOI:10.32397/tesea.vol6.n2.648

and disturbances. This implies that controlling key concerns might be managed using the concept of a micro-grid in grid-connected or standalone mode, which can be addressed to enhance and regulate the frequency of the system in vast industrial and regional areas. Other ways of ensuring consistent supply of electricity inside the electrical infrastructure can be supported by diesel-generating and wind-powered units, which have gained popularity due to renewable energy sources in restricted control systems. Wind-based units are vulnerable to swings in production and the frequency of the system owing to variability in the wind velocity or in load demand, which affects the frequency of the system and hence in [5], author proposed a model that utilised a snake optimization tuning method of the PID control system. In [6], the author have come up with a hybrid fuel cell–photovoltaic generator model and result verifies SPV-hydrogen energy production in a stand-alone system. The model, control technique and power adjustment of mixed PV-fuel cell with battery energy storage system (BESS) supplying electric vehicle was shown in [7]. In [8], authors have used various sources such as SPV, wind, BESS and fuel cells for parallel operation and control strategy was developed. The combination of PV-Wind with BESS system feeding a load using inverter was successfully shown in [9]. The modeling and entertainment of a micro-grid based renewable control system was discussed in [10] and it comprises of wind turbine, doubly fed induction generator, PV generator, fuel cell and BESS. Usually, RES were dictated by prevailing weather conditions, particularly when the energy demand surpassed the supply capacity. In the event of a surplus of power, where the supply exceeds the demand, RES facilities need to effectively handle the excess by employing Energy Storage Devices (ESD). These ESDs can manage and regulate the surplus supply for a specified duration as the load increases; subsequently, the demand would deplete the stored energy in the ESDs based on the system's needs.

Energy storage devices, such as batteries, capacitors, flywheels, and superconducting magnet energy storage (SMES), play a crucial role in managing energy surges and delivering it during peak load demands [11–22]. Among these, energy storage devices working in conjunction with the hydrogen generative aqua electrolyzer (HAE) – incorporating a fuel cell – are deemed more capable compared to other ESDs due to their operational requirements. Renewable Energy Sources (RES), capable of accommodating various energy storage methods, can leverage the HAE system to decompose water or natural gas into oxygen and hydrogen. The compressed gas can then be stored, with subsequent transportation through pipelines to fuel cells. In cases of substantial demand, the HAE has the potential to regulate the system status [17, 18]. The RFB is another quick storage appliance in the system, which is especially helpful when generator rotors require lead time owing to regulating demand. The RFB can reduce electromechanical irregularities in control systems by discharging via inverter/rectifier networks. This versatility enables the RFB to respond quickly to load variations, effectively decreasing the strain on the system [19, 20]. Likewise, ultra-capacitors (UC) have become powerful and cheaper storage devices currently and plaid by number of investigators for diverse electrical uses and hence these diverse ESD plays a crucial role in enhancing the efficiency of diesel-wind isolated systems.

Whether it is a system with higher capacity such as centralized power stations or reduced capacity system such as a diesel-wind isolated system known as microgrid, Frequency regulation is an important aspect of electricity transmission networks to be met by today's customers and hence it is very important to maintain the equilibrium between the electrical energy generation with the load demand in the microgrid. The frequency will be also affected in case the wind speed changes. The mismatch between energy generation and load demand will result in shifting the frequency from nominal value and that is why microgrid needs the simplest and effective control strategies to regulate the frequency as well as power output of wind turbine generator. The PID controllers are one of the simplest and straightforward designs and very common in almost all the power and control industries [23]. The PID controllers has proportional, integral and derivative actions and work as feedback controllers to manage the mismatches between the actual and desired output. To improve the output of PID, an effective tuning technique is a must, and researchers

have proposed various tuning techniques to improve the response of a PID controllers. Zeigler-Nichol's method is one of the first choice of researchers and industry engineers to find the gains of PID to improve the dynamic performance of the microgrid for various working conditions. Considering the preceding discussion, this study is intended to attain the following:

- Shows a detailed model of a diesel-wind isolated system, otherwise known as a microgrid, which can provide uninterrupted electrical energy to smaller communities. This model combines conventional and renewable energy sources and was developed using a transfer function approach for research and investigation purposes.
- Demonstrates how the comprehensive modeling of various energy storage devices, including UC, HAE-FC, RFB, SMES, and BESS, can be used to assess their impact on microgrids.
- Exhibit and verify diverse PIDs such as classic-PID, Pessen Integral Rule-PID, some overshoot-PID and there is no overshoot-PID for microgrids, thus frequency and power variations are reduced in the occurrence of changes in load or an alteration in wind velocity.
- Demonstrates the performance of various PIDs under similar working conditions and to find the best design of PID for the operation of microgrid. Three different error definitions; integral time multiplied absolute error (ITAE), integral absolute error (IAE) and integral time multiplied square error (ITSE) are used to evaluate the performance of various PIDs.
- From the simulation results, it is seen that Pessen Integral Rule-PID provides promising results in view of minimum error values and in view of minimized system deviations and hence research work is extended to see the impact of various ESDs with one at a time in the microgrid with Pessen Integral Rule-PID.
- The results of different ESDs are compared for an incremental variation in load and wind velocity and the application results are shown to see the best ESD for microgrid considering error values and system responses.

2. Detailed Modelling of the Microgrid

Wind turbines and diesel generators (DEG) are two of the most trustworthy sources of energy for assuring regular electricity delivery. The DEG and WTG standalone generating systems have a maximum output of 150 KW. Because the WTG is reliant on atmospheric factors, specifically the speed of the wind, the DEG has a benefit in providing continuous electrical power. Figure 1 depicts the linear representation of DEG. The model is fed by a DEG that features a turbine and a speed governor. The transfer function is represented below [4]:

$$\Delta P_{GD} = \frac{1}{(1+sT_{D4})}\Delta P_{GT} \tag{1}$$

$$\Delta P_{GT} = \left(\frac{K_D(1+sT_{D1})}{(1+sT_{D2})(1+sT_{D3})}\right)\Delta P_G \tag{2}$$

$$\Delta P_G = \Delta P_{CD} - \left(\frac{1}{R_D}\right)\Delta F \tag{3}$$

As the speed governor serves as the model's eye, ΔP_{GT} adjusts the governor's output (p.u.) and sends a control signal to the diesel system (p.u.). ΔP_G delivers the control signal of the speed governor (p.u.). ΔF represents the change in frequency, K_D stands for the gain of the speed governor, and T_{D1}, T_{D2}, and T_{D3} signify the time constants (sec). The turbine is characterized by a unity gain and a responding time. T_{D4} is also a speed regulator represented by R_D of the diesel system. The WTG system transforms the

kinetic energy of the wind into electricity via mechanical phenomenon. In the WTG framework, the shift from hydraulic linkage to actual speed necessitates a distinction between turbine and generator frequencies. Equation (4) delineates the change in generated power [4]:

$$\Delta P_{WTG} = K_{IG} \left[\Delta F_T - \Delta F\right] \tag{4}$$

ΔF_T signifies the variation in speed of wind generator, and K_{IG} denotes the gain from the hydraulic connection. The speed of the induction generator can be mathematically written using Equation (5):

$$\Delta F_T = \left(\frac{1}{1+sT_W}\right) \left[K_{TP}\Delta F_T - \Delta P_{WTG} + K_{PC}\Delta X_3 + \Delta P_{IW}\right] \tag{5}$$

In most wind energy production strategies, blade properties must be examined. K_{PC} symbolizes the blade gain contribution, ΔP_{IW} represents the input wind control. The data fit pitch (DFP) yield is considered with ΔX_3 within the system. Most systems require some lag compensation, which uses an effect to correspond with the gain features of the microgrid concept. The DFP yield can be expressed as:

$$\Delta X_3 = \Delta X_2 \left[\frac{K_{P3}}{1+sT_{P3}}\right] \tag{6}$$

Where, ΔX_2 represents the yield of hydraulic pitch and the system also considers the responding time of the DFP with T_{P3}, a gain indication with K_{P3}. The hydraulic pitch system (HPS) regulates the pitch angle of the blades. It produces an output of:

$$\Delta X_2 = \Delta X_1 \left[\frac{K_{P2}}{1+sT_{P2}}\right] \tag{7}$$

In Equation (7), ΔX_1 represents the yield of the pitch controller, K_{P2} indicates the HPS gain, and T_{P2} represents the HPS time constant. The pitch angle must be thoroughly evaluated for the wind turbine to produce the highest possible production. The pitch angle systems are represented as follows:

$$\Delta X_1 = \Delta P_{CW} \left[\frac{K_{P1}(1+sT_{P1})}{1+s}\right] \tag{8}$$

Equation (8) gives a command signal (p.u.) of the pitch angle system by ΔP_{CW} and K_{P1}, indicating the gain of the pitch angle output. T_{P1} enables the pitch angle mechanism to adjust in seconds, providing control and gain to the system. The quality of power produced by the microgrid necessitates frequency limitation in the entire system, which must consider the load demand for the DEG and WTG systems to create total power. Having stated that, any miscommunication between the produced control and load request may cause variations in the microgrid frequency, which must be regulated effortlessly as feasible. As shown in Equation (9), the microgrid frequency response generates a first-order representation consisting of gain, transfer function, and time constant. K_P indicates the gain, and T_P indicates the microgrid's time constant, as seen below:

$$\Delta F = \Delta P_{IDWS} \left[\frac{K_P}{1+sT_P}\right] \tag{9}$$

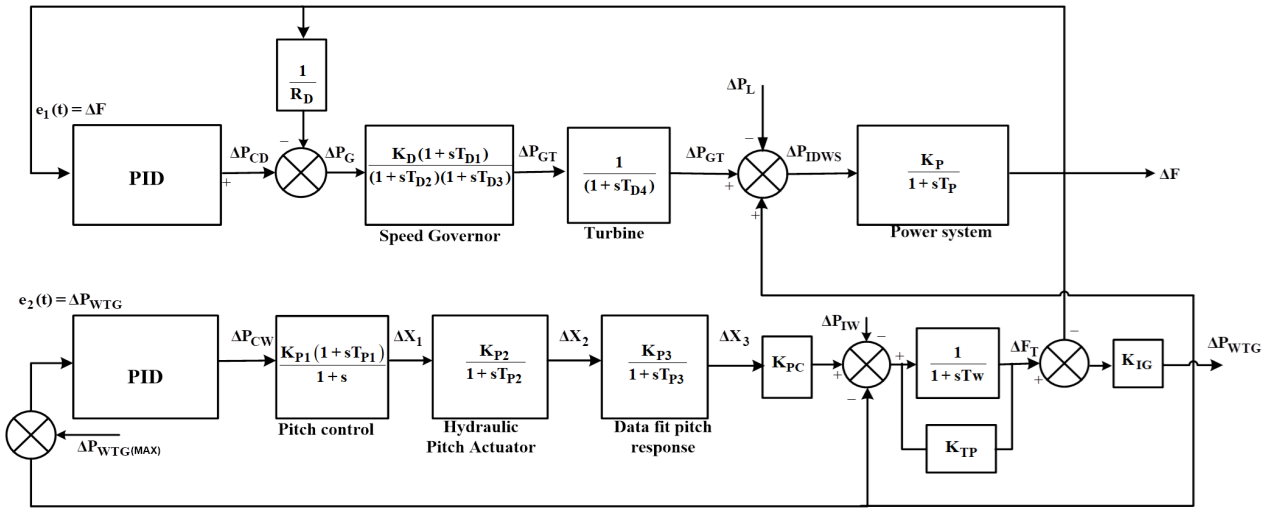

Figure 1. Model of a Microgrid.

3. Modelling of Superconducting Magnetic Energy Storage (SMES)

SMES units contain static components comprising a superconducting coil element, a refrigeration-vacuum unit and a power conditioning unit. This device stores electrical energy within the magnetic coil, obtained from the interconnected network. Once electrical energy is required, a substantial amount of energy can be transferred in a relatively small amount of time. This discharge of electrical energy quickly also allows the system to avoid huge losses. During normal power grid operation, the magnetic coil is charged up to a predetermined level linked to the power grid by a power conversion system. When the load demand suddenly weighs on the coil, the stored energy is released back into the AC grid by the power conversion system. The coil charges to its initial state after the required demand has been met. Equation (10) below relates to the transfer function of the SMES system and Figure 2 shows the schematic representation of SMES as used for investigations [11, 12].

$$G_{SMES}(s) = \frac{K_{SMES}}{1 + sT_{SMES}} \tag{10}$$

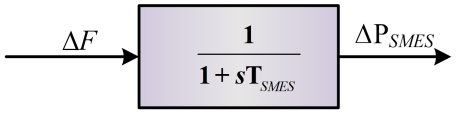

Figure 2. Transfer Function of SMES.

4. Modelling of Ultra Capacitor (UC)

Sophisticated electrical devices technology has emerged in the electrochemical device category, specifically ultra-capacitors (UCs), sometimes known as electric double-layer capacitors or super capacitors. A UC has two permeable anodes separated by an ion-exchange layer and an electrolyte composed of potassium hydroxide. The permeable connections and electrolytic fluid have a much larger area of surfaces than a typical capacitor. UCs also stand out for their higher capacitance due to the slightly broader two-fold layer that is between the capacitors. Two aspects that boost the durability of UCs with a multiplication

factor of almost 10 times that of a typical electrolytic capacitor. UCs' lightweight and substantial energy density offer them an advantage over ordinary capacitors, allowing for a considerable amount of energy to be stored. While most UCs have a higher power capacity than batteries, they also have a significant 1–10 Wh/kg rating of specific energy and 1000–5000 W/kg of specific power energy rating. They may be drained and recharged more quickly than a BESS or standard capacitors, and they require no upkeep and have an increased life span. The properties of a UC make it acceptable for an extensive variety of LFCs, irregularities may be managed by various hypotheses, and a UC can be validated using a first-order TF. A control zone frequency deviation may be used as an input to the UC, and its TF is illustrated in Equation (11) [14, 15]:

$$\Delta P_{UC}(s) = \left\{ \frac{K_{UC}}{1 + sT_{UC}} \right\} \Delta F(s) \tag{11}$$

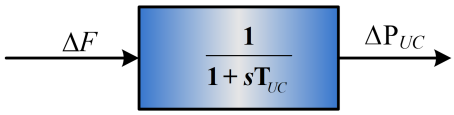

Figure 3. Schematic of UC.

KUC refers to the gain pick time of a UC, and TUC denotes the time constant. The gain KUC is determined by the state of charge (SOC). It is important to note that the UC's gain is consistently kept within the range of 50 to 90 percent within the operational SOC. This modelled transfer function of the UC is illustrated in Figure 3.

5. Modelling of Hydrogen Aqua Electrolyzer-Fuel Cell (HAE-FC)

Hydrogen is one of the most viable alternative energy sources used as an electrical carrier. Hydrogen has previously supplanted other fuels in fixed power plants used to generate electricity in a variety of sectors. The hydrogen structure consists of an electrolyzer unit for converting input electrical energy into hydrogen by cutting down water particles, the hydrogen capacity structure, and the hydrogen energy transformation arrangement, which converts the chemical energy stored inside the hydrogen back into electricity, as shown in Figure 4.

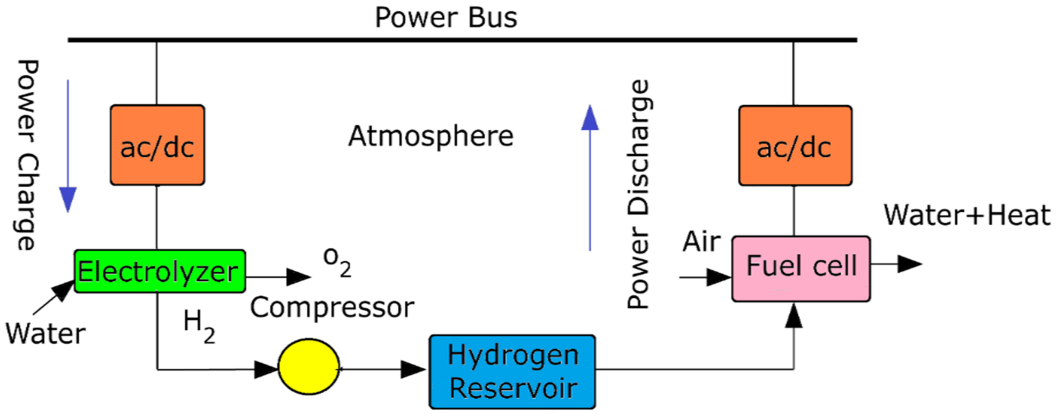

Figure 4. Operational Method of HAE-FC.

Most of the hydrogen collected is used to generate energy, which includes fuel cell support. The exchange work shape of the aqua electrolyzer can be formed using equation (12) [17] and schematic model of HAE is shown in Figure 5.

$$G_{AE}(s) = \frac{K_{AE}}{1 + sT_{AE}} \tag{12}$$

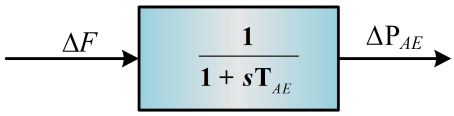

Figure 5. Transfer Function of HAE.

Fuel cells are passive equipment that convert the chemical vitality of fuel, specifically hydrogen, into electricity. Because of their exceptional efficiency and lack of contaminants, they are an important energy source asset in a distributed control system. Equation (13) can be used to calculate the fuel cell's exchange work:

$$G_{FC}(s) = \frac{K_{FC}}{1 + sT_{FC}} \tag{13}$$

Figure 6. Transfer Function of FC.

6. Modelling of Redox Flow Battery

The Redox flow battery (RFB) is a vital energy storage technology with a quick response to frequency changes. The reaction speed indicator of the RFB can adjust its operational time in seconds. It is more efficient because of its substantial charging and discharging capability. The RFB has a unique characteristic in that the electrolyte is kept in two separate tanks. This characteristic prevents self-discharge of the RFB, resulting in a substantially longer life expectancy as compared to similar ESDs. One of the brief descriptors of RFB is in which a solution that contains electrolytes such as sulfuric acid and vanadium ions, which are contained in both a positive and negative tank. Additionally, the RFB operation is safe at standard temperatures, despite its reputation for quick charging and discharging. Another advantage of the RFB is the capability to reload efficiently following a load disruption. This implies that the set value of the RFB can be promptly reset to prevent interruptions during subsequent load disruptions. The deviating frequency signal would determine the value of RFBs, and the amount of power exchanged with the system. The RFB is a rechargeable battery whose life is not harmed by repeated charging or discharging, and it responds fast to unexpected load changes. When it pertains to load levelling, the RFB is more important. It helps to maintain the quality of the power. Figure 7 depicts the model of the RFB derived from [21].

$$\Delta P_{RFB}(s) = \left\{ \frac{K_{RFB}}{1 + sT_{RFB}} \right\} \Delta F(s) \tag{14}$$

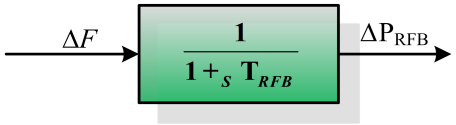

Figure 7. Transfer Function of RFB.

7. Modelling of Battery Energy Storage System

Battery energy storage system (BESS) has been integrated due to the advantage of having a large energy density and fast access time. Another positive side to the BESS is it provides proper storage of wind energy. This advanced technology allows the grid to be linked and powered with a bank of batteries and a converter. Most Battery Energy Storage Systems (BESS) consist of lead-acid battery installations, providing a significant level of operational flexibility and a relatively swift response time. A feasible combination within the BESS structure would be to have a series-parallel connection. Most plants incorporated with BESS benefit from an immediate power reserve and electric power for frequency management. These advantages in the plant assist with the reduction in peak power demand. Amongst ES devices the BESS has one of the highest time constants, due to the time taken to charge the battery cell. The transfer function of BESS can be characterized by Equation (15) [22], and schematic model is shown in Figure 8.

$$G_{BESS}(s) = \frac{K_{BESS}}{1 + sT_{BESS}} \tag{15}$$

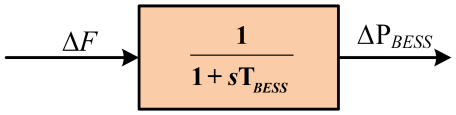

Figure 8. Transfer Function of BESS.

8. Design and Modelling of Diverse PIDs

The broad aspect of control systems can be categorized in two, open-loop control and closed-loop control. Within open-loop control systems there is no feedback, which makes the controller responsible for independently sending a signal to the actuator. In a closed-loop system, feed-back is continuously considered so the controller can make the required adjustments and to keep the output stable and where it belongs. A basic block diagram of a closed loop system is illustrated in Figure 9.

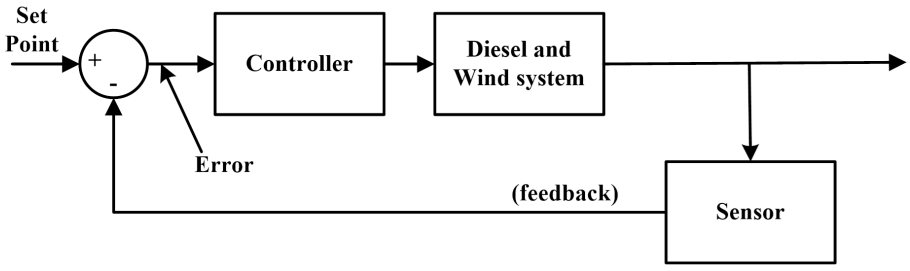

Figure 9. PID-Closed-loop control system.

The numerical description of a PID controller is given in Equation (16):

$$K_pE + K_IK_p\sum(E\Delta t) + K_DK_p\frac{\Delta E}{\Delta t} \tag{16}$$

where K_p = proportional gain, K_I = integral gain, and K_D = derivative gain.

The three-loop control with feedback of the PID method is a unique feature that can achieve an optimal output after a system has been disturbed. The methods' main input is the feedback of the error value that is utilized to reconfigure the desired and the actual values of the system. The error value within the system is multiplied with the gain (K) to form the proportional term. Within the controller, a large and positive error would also influence a large and positive output which includes the value of gain K. This outlines the significance of gain K in the reduction of overshoot within the system's response. The system response steady-state error can be eliminated by integrating the actual and desired response into the integral loop over time, as the PI would not be able to eliminate the error. Lastly, the derivative control is applied as this would take into consideration the rate of change of error. This intern would assist in the reduction of oscillations and assist in the improvement of the damping conditions within the system response. Figure 10 below illustrates the PID structure.

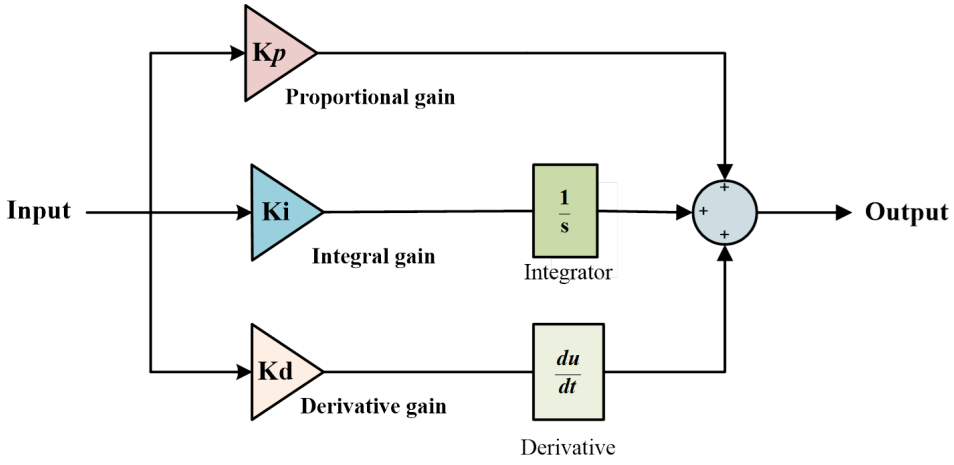

Figure 10. PID Structure.

Further, the PID controllers need tuning methods and in the present research work, the Nichols Method (ZNM) [23] is used to fine tune the gains of various PIDs. Three distinct error definitions are employed to assess the output of different PID controllers in the context of a microgrid responding to a specific disturbance. These measures include the Integral of Time-weighted Absolute Error (ITAE), the Integral of Time-weighted Square Error (ITSE), and the Integral of Absolute Error (IAE) as per equations (17), (18), and (19).

IAE produces sluggish characteristics. On the other hand, ITSE can give a quick dynamical response, but it causes significant prolonged vibrations due to squaring and bearing the inaccuracy at the beginning of the reaction. Introducing a time weighting factor to IAE leads to the attainment of ITAE, culminating in a more satisfactory response characterized by a faster settling time and minimal overshooting. The mathematical representation of these error definitions is given by Equations (17), (18), and (19) which follows below:

$$ITAE = \int_0^{ts} t\,|\Delta F|\,dt \tag{17}$$

$$IAE = \int_0^{ts} |\Delta F| \, dt \tag{18}$$

$$ITSE = \int_0^{ts} |\Delta F|^2 \, t \, dt \tag{19}$$

9. Simulation Results and Analysis

This research work discusses the importance and mathematical modelling of microgrids in an interconnected arrangement having DG and WTG. The DG is equipped with a speed governor setting and responsible for variation in electricity production of the microgrid as per the present demand of the customers connected to the microgrid. The microgrid also consists of a WTG where power will be generated through the energy of the wind, and it is connected to DG so that the microgrid is an amalgamation of conventional and non-traditional energy sources that can meet the electric power needs of an isolated neighborhood or consumer group. Due to varying consumer patterns, the load demand of the microgrid will change over time and hence the frequency of the system will fluctuate and affect the microgrid customers. On the other side, due to change in wind speed, frequency will fluctuate. Therefore, an effective controller must be designed to cope with the frequency and power deviations. Hence, this article discusses the design and analysis of diverse PID controllers for frequency stabilization of the microgrid. This work also discusses the design and modelling of ESD such as SMES, BESS, HAE-FC, UC and RFB and it can be perceived that these ESD are having the potential to enhance the performance of the microgrid in the event of sudden load changes or sudden changes in the wind speed which will all for the stabilization of the operation within microgrid much faster.

First, the four diverse PID structures are selected, i.e., Classic PID, Pessen Integral Rule, Some Overshoot and No Overshoot, to minimize the microgrid frequency and power deviations and hence to stabilize the behavior of the microgrid.

The conventional PID controllers require tuning to fine tune their gains to achieve the desired output and hence the well-known Z-N tuned method is used to fine tune the gains of various PIDs. To achieve gains through Z-N method, the first step is to calculate ultimate gain (Ku) and ultimate time (Tcr). The ultimate gain Ku = 0.16 and Tcr = 5.208 is evaluated as per Z-N method for DG and Ku = 0.2 and Tcr = 4.1666 calculated for WTG. The next step is to calculate the gains of various PIDs, and these can be found through data given in Table 1. The calculated gains for various PIDs for DG are shown in Table 2 and for WTG is shown in Table 3. After calculating the gains of various PIDs, the next step is to check the output of these PIDs for microgrid in the wake of step change in the load (0.01 p.u.) in the microgrid. The output of various PIDs is obtained by calculating three error definitions which are ITAE, IAE and ITSE. These standard error definitions are of utmost importance in obtaining and understanding the capability of individual controller to minimize the microgrid deviations and hence the better controller should be capable enough to give minimum value of ITAE, IAE and ITSE for a particular disturbance. The ITAE, IAE and ITSE numerical values obtained via Pessen Integral Rule is much lesser when matched with numerical values of other PIDs. Further, the ITAE, IAE and ITSE values of classic PID is also less in comparison to Some overshoot PID and No overshoot PID and hence it is seen that Pessen Integral Rule PID is efficacious in reducing the error values.

Figure 11 (a-b) displays the plotted outcomes for an adjustment in load demand of 0.01 p.u. and it is seen that all PIDs experiences higher overshoot and the PID responses are not able to settle within 50 seconds also for ΔF and ΔP_{WTG} results. Still, the results of Pessen Integral Rule PID show minimum overshoot and trying to reach zero position much faster in comparison to other PIDs. In the next step, an 0.01 p.u. alteration in the wind speed with respect to normal speed is applied in WTG and the responses

of ΔF and ΔP_{WTG} are recorded and shown for various PIDs through Figure 12 (a-b). The look at results shows that PIDs are struggling to minimize overshoot, unable to settle to steady-state position with larger settling time. However, the results of microgrid deviations obtained by Pessen Integral Rule PID is better in comparison to other PIDs in terms of lesser overshoot but it is imperative for the controller to obtain reduced overshoot, less settling time, and zero-steady state error and hence Pessen Integral Rule PID is chosen for further analysis with impact of various ESD in the microgrid for frequency stabilization studies. The obtained value of IAE, ITSE and ITAE for Pessen Integral Rule (PIL) PID with impact of various ESDs for 0.01 p.u. change in the load demand is shown in Table 4.

The results of Table 5 clearly reveal that each ESD has the capability to reduce the ITAE, IAE and ITSE when matched with PIL only. The PIL has (ITAE: 19.81, IAE: 0.6124 & ITSE: 0.1246) whereas PIL + UC has (ITAE: 17.39, IAE: 0.4055 & ITSE: 0.06416). The PIL + BESS has (ITAE: 19.84, IAE: 0.6116 & ITSE: 0.1243), PIL + HAE-FC (ITAE: 19.87, IAE: 0.6098 & ITSE: 0.1234), PIL + SMES (ITAE: 18.65, IAE: 0.4535 & ITSE: 0.07607) and PIL + RFB (ITAE: 0.03233, IAE: 0.01584 & ITSE: 0.000071). From all ESDs, it is seen that RFB is much better and advanced to minimize the three diverse error definitions to minimum value. The results of BESS and HAE-FC are almost comparable for microgrid. However, results of UC are better than BESS, HAE-FC and SMES but not better than RFB. The dynamic performance of PIL with all ESDs are obtained and shown through Figure 13 (a-b). The look at graphical results of ΔF and ΔP_{WTG} clearly shows that PIL + RFB outperforms all other ESDs. The first peak is less, and the system settles back to original value within couple of seconds. The trend of settling is smooth. The results of PIL with UC are also promising. Further the results of other ESDs with PIL offer higher overshoot and steady state error. The system responses are not able to reach a steady state position within 50 seconds also and hence PIL with RFB outperforms all other ESDs for microgrid. Table 6 shows IAE, ITSE and ITAE for PIL- PID with Impact of ESDs for 0.01 p.u. change in wind speed from the normal speed and here also PIL with RFB reduces the error values in comparison to values achieved through PIL with other ESDs. The microgrid deviations are shown by Figure 14 (a-b) and it is seen that RFB performs much better in achieving all quality of system responses in comparison to other ESDs. This is due to fact that responding time of RFB is zero seconds and hence much faster to improve the dynamic performance of the microgrid.

Table 1. Gains calculation criteria for different PIDs.

Controller Structure	K_p (Proportional Gain)	K_i (Integral Gain)	K_d (Derivative Gain)
Classic PID	$0.6\,Ku$	$1.2\,Ku/Tu$	$3\,Ku\,Tu/40$
Pessen Integral Rule	$7\,Ku/10$	$1.75\,Ku/Tu$	$21\,Ku\,Tu/200$
Some Overshoot	$Ku/3$	$0.666\,Ku/Tu$	$Ku\,Tu/9$
No Overshoot	$Ku/5$	$0.4\,Ku/Tu$	$Ku\,Tu/15$

Table 2. Gains calculated for different PIDs for DG.

Controller Structure	K_p (Proportional Gain)	K_i (Integral Gain)	K_d (Derivative Gain)
Classic PID	0.096	0.0368	0.0624
Pessen Integral Rule	0.112	0.0537	0.0874
Some Overshoot	0.0533	0.0204	0.0925
No Overshoot	0.032	0.0122	0.0555

Table 3. Gains calculated for different PIDs for WTG.

Controller Structure	K_p (Proportional Gain)	K_i (Integral Gain)	K_d (Derivative Gain)
Classic PID	0.12	0.0576	0.06249
Pessen Integral Rule	0.14	0.0840	0.0874
Some Overshoot	0.0666	0.0319	0.0925
No Overshoot	0.04	0.0192	0.0555

Table 4. IAE, ITSE and ITAE values achieved for different PIDs.

Controller Structure	IAE	ITSE	ITAE
Classic PID	0.7981	0.23	31.01
Pessen Integral Rule	0.6124	0.1246	19.81
Some Overshoot	1.058	0.4712	47.51
No Overshoot	1.227	0.697	58.66

Table 5. IAE, ITSE and ITAE for PIL- PID with Impact of ESDs for 0.01 p.u. alteration in the load demand.

PID with ESD	IAE	ITSE	ITAE
Pessen Integral Rule (PIL)	0.6124	0.1246	19.81
PIL + UC	0.4055	0.06416	17.39
PIL + BESS	0.6116	0.1243	19.84
PIL + HAE-FC	0.6098	0.1234	19.87
PIL + SMES	0.4535	0.07607	18.65
PIL + RFB	0.01584	0.000071	0.03233

Table 6. IAE, ITSE and ITAE for PIL- PID with Impact of Energy Storage Devices for 0.01 p.u. change in wind speed from normal speed.

PID with ESD	IAE	ITSE	ITAE
Pessen Integral Rule (PIL)	0.2335	0.02292	7.452
PIL + UC	0.148	0.008987	6.01
PIL + BESS	0.2328	0.0228	7.432
PIL + HAE-FC	0.2314	0.02251	7.379
PIL + SMES	0.1648	0.01089	6.341
PIL + RFB	0.009053	0.000021	0.1884

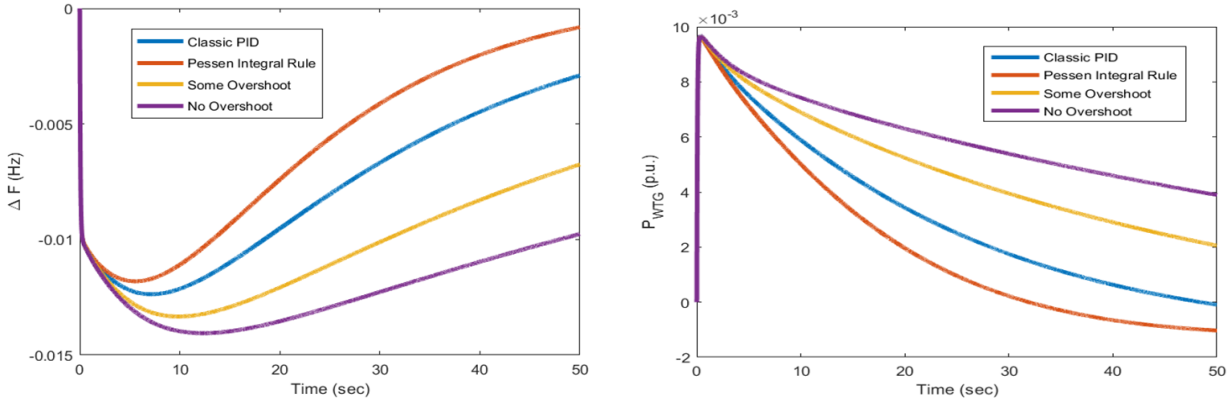

(a) **(b)**

Figure 11. Output matched for diverse PID controllers for 0.01 p.u. change in load alteration.

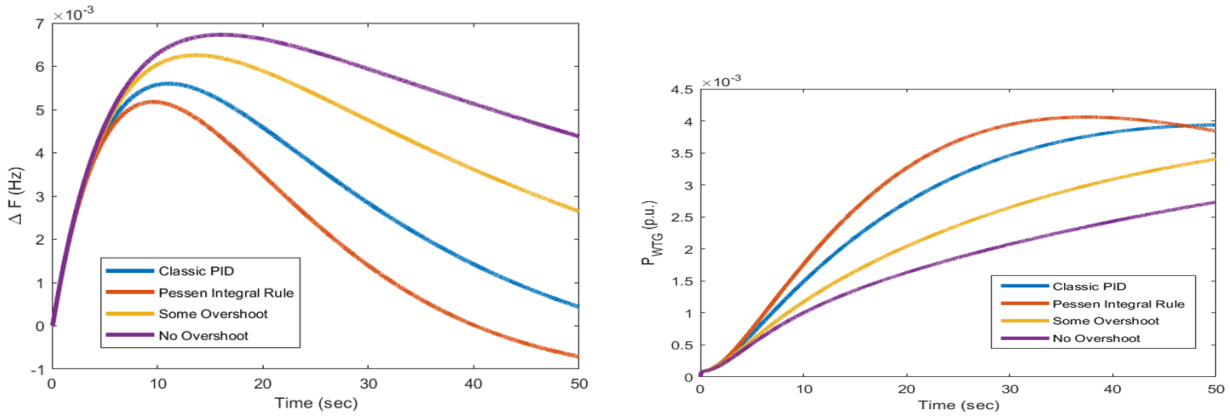

(a) **(b)**

Figure 12. Output matched for diverse PID controllers for 0.01 p.u. alteration in wind speed from original speed.

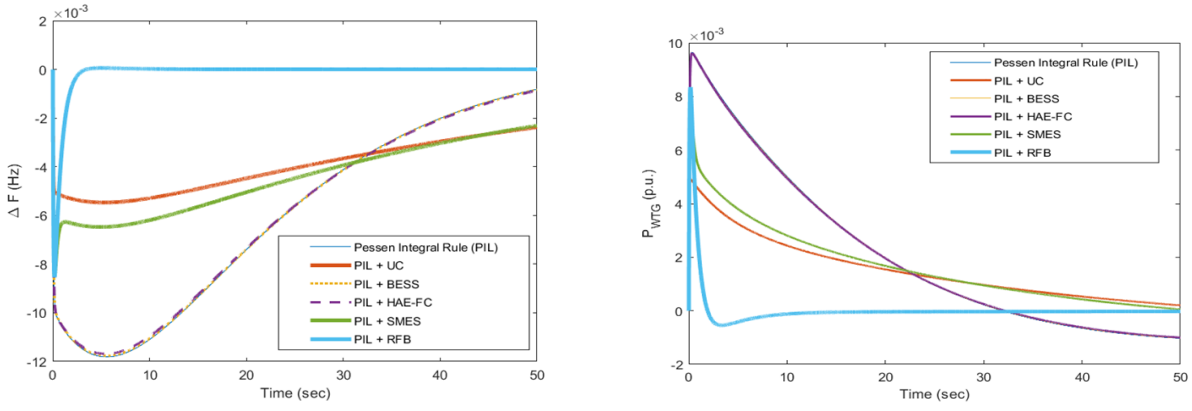

(a) **(b)**

Figure 13. Output matched for PIL-PID with impact of various storage devices in diesel-wind system and obtained for 0.01 p.u. step change in the load alteration.

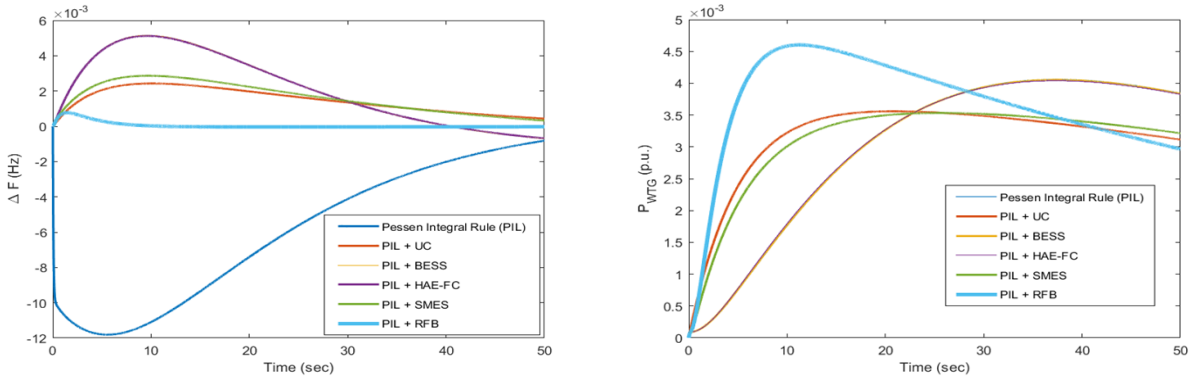

(a) **(b)**

Figure 14. Output matched for PIL-PID with the effect of various storage devices in a diesel-wind system and obtained for 0.01 p.u. alteration in wind speed with respect to normal speed.

10. Conclusions

This presents work discusses the detailed mathematical modelling of the microgrid having DG and WTG. In addition, the modelling of diverse ESDs is also presented. This work also discusses the design of different PIDs and their capability to reduce the deviations in frequency and power of the microgrid in view of various working conditions. Three error definitions are utilized to assess the effectiveness of different PIDs. The investigations reveal that PIL-PID can minimize the frequency and power deviations of the microgrid. However, there is a possible scope for the enhancement and therefore, diverse ESDs are studied and implemented to enhance the performance of the microgrid. The numerical and graphical outcomes verify that PIL-PID with RFB outperforms over other ESDs. The outcome of PIL-PID with UC is also promising but not better than PIL-PID with RFB.

Funding: This research received no external funding

Author contributions: The Conceptualization, V.R.; Methodology, V.R. and G.S.; Software, V.R.; Validation, V.R., M.B. and P.N.B.; Investigation, V.R.; Writing – Original Draft Preparation, V.R. and M.B.; Writing – Review & Editing, V.R. and M.B.; Supervision, G.S. and P.N.B. All authors have reviewed, discussed, and agreed to their individual contributions.

Disclosure statement: The authors declare no conflict of interest.

References

[1] Hêmin Golpîra, Arturo Román-Messina, and Hassan Bevrani. *Renewable Integrated Power System Stability and Control*. Wiley, March 2021.

[2] Emre Çelik, Nihat Öztürk, Yogendra Arya, and Cemil Ocak. (1+pd)-pid cascade controller design for performance betterment of load frequency control in diverse electric power systems. *Neural Computing and Applications*, 33(22):15433–15456, June 2021.

[3] Emre Çelik. Design of new fractional order pi–fractional order pd cascade controller through dragonfly search algorithm for advanced load frequency control of power systems. *Soft Computing*, 25(2):1193–1217, August 2020.

[4] Somnath Ganguly, Chandan Kumar Shiva, and V. Mukherjee. Frequency stabilization of isolated and grid connected hybrid power system models. *Journal of Energy Storage*, 19:145–159, October 2018.

[5] Emre Çelik. Exponential pid controller for effective load frequency regulation of electric power systems. *ISA Transactions*, 153:364–383, October 2024.

[6] Djamila Rekioua, Samia Bensmail, and Nabila Bettar. Development of hybrid photovoltaic-fuel cell system for stand-alone application. *International Journal of Hydrogen Energy*, 39(3):1604–1611, January 2014.

[7] Zahra Mokrani, Djamila Rekioua, and Toufik Rekioua. Modeling, control and power management of hybrid photovoltaic fuel cells with battery bank supplying electric vehicle. *International Journal of Hydrogen Energy*, 39(27):15178–15187, September 2014.

[8] N. Mezzai, D. Rekioua, T. Rekioua, A. Mohammedi, K. Idjdarane, and S. Bacha. Modeling of hybrid photovoltaic/wind/fuel cells power system. *International Journal of Hydrogen Energy*, 39(27):15158–15168, September 2014.

[9] S. Aissou, D. Rekioua, N. Mezzai, T. Rekioua, and S. Bacha. Modeling and control of hybrid photovoltaic wind power system with battery storage. *Energy Conversion and Management*, 89:615–625, January 2015.

[10] S. Tamalouzt, N. Benyahia, T. Rekioua, D. Rekioua, and R. Abdessemed. Performances analysis of wt-dfig with pv and fuel cell hybrid power sources system associated with hydrogen storage hybrid energy system. *International Journal of Hydrogen Energy*, 41(45):21006–21021, December 2016.

[11] Emre Çelik and Nihat Öztürk. Novel fuzzy 1pd-ti controller for agc of interconnected electric power systems with renewable power generation and energy storage devices. *Engineering Science and Technology, an International Journal*, 35:101166, November 2022.

[12] Sayed M. Said, Emad A. Mohamed, Mokhtar Aly, and Emad M. Ahmed. *Enhancement of load frequency control in interconnected microgrids by SMES*, page 111–148. Institution of Engineering and Technology, December 2022.

[13] Emre Çelik, Nihat Öztürk, and Essam H. Houssein. Improved load frequency control of interconnected power systems using energy storage devices and a new cost function. *Neural Computing and Applications*, 35(1):681–697, September 2022.

[14] Arindita Saha and Lalit Chandra Saikia. Performance analysis of combination of ultra-capacitor and superconducting magnetic energy storage in a thermal-gas agc system with utilization of whale optimization algorithm optimized cascade controller. *Journal of Renewable and Sustainable Energy*, 10(1), January 2018.

[15] Arindita Saha and Lalit Chandra Saikia. Utilisation of ultra-capacitor in load frequency control under restructured stpp-thermal power systems using woa optimised pidn-fopd controller. *IET Generation, Transmission amp; Distribution*, 11(13):3318–3331, September 2017.

[16] Shemin Sagaria, Rui Costa Neto, and Patricia Baptista. Assessing the performance of vehicles powered by battery, fuel cell and ultra-capacitor: Application to light-duty vehicles and buses. *Energy Conversion and Management*, 229:113767, February 2021.

[17] Yogendra Arya. Impact of hydrogen aqua electrolyzer-fuel cell units on automatic generation control of power systems with a new optimal fuzzy tidf-ii controller. *Renewable Energy*, 139:468–482, August 2019.

[18] Issarachai Ngamroo. Application of electrolyzer to alleviate power fluctuation in a stand alone microgrid based on an optimal fuzzy pid control. *International Journal of Electrical Power amp; Energy Systems*, 43(1):969–976, December 2012.

[19] R. Francis and I.A. Chidambaram. Optimized pi+ load–frequency controller using bwnn approach for an interconnected reheat power system with rfb and hydrogen electrolyser units. *International Journal of Electrical Power amp; Energy Systems*, 67:381–392, May 2015.

[20] Maninder Kaur, Sandeep Dhundhara, Sanchita Chauhan, and Mandeep Sharma. Lithium-ion vs. redox flow batteries – a techno-economic comparative analysis for isolated microgrid system, September 2021.

[21] Rabindra Kumar Sahu, Tulasichandra Sekhar Gorripotu, and Sidhartha Panda. A hybrid de–ps algorithm for load frequency control under deregulated power system with upfc and rfb. *Ain Shams Engineering Journal*, 6(3):893–911, September 2015.

[22] Emre Çelik, Nihat Öztürk, and Essam H. Houssein. Influence of energy storage device on load frequency control of an interconnected dual-area thermal and solar photovoltaic power system. *Neural Computing and Applications*, 34(22):20083–20099, July 2022.

[23] Avinash Panwar, Vinesh Agarwal, and Gulshan Sharma. Frequency control studies of hydro system using ai applications. In *2021 International Conference on Artificial Intelligence, Big Data, Computing and Data Communication Systems (icABCD)*, page 1–5. IEEE, August 2021.